02

Study of spectral dependence of fluorescence lifetime of acridine orange in one-dimensional photonic crystals

© Yu.A. Strokova, S.E. Svyakhovsky, A.M. Saletsky

Department of Physics, Moscow State University,
Moscow, Russia

e-mail: sam@physics.msu.ru

Received August 31, 2024 Revised August 31, 2024 Accepted September 30, 2024

The spectral dependences of fluorescence intensity I and average lifetime of excited state τ of acridine orange (AO) molecules embedded in one-dimensional photonic crystals (PC) at different radiation detection angles were studied. The density of electromagnetic modes of PC was calculated using the scattering matrix method. The spectral characteristics of AO fluorescence in PC samples and samples with permanent pores (porous silicon) were compared, as well as with the calculated dependences of the relative density of electromagnetic modes.

The kinetics of AO fluorescence decay in PC were studied at different wavelengths, which were approximated by two exponentials. It was found that short-term luminescence is practically independent of the wavelength, while for long-term luminescence a non-monotonic dependence on λ is observed with a minimum corresponding to the photonic band gap. The Purcell factor was estimated for the studied systems. It was proven that the experimentally obtained dependences of the energy and time characteristics of AO fluorescence on λ are due to a change in the density of photonic states.

Keywords: photonic crystals, photonic band gap, density of electromagnetic modes, acridine orange, fluorescence spectra, fluorescence lifetime.

DOI: 10.61011/EOS.2024.09.60037.7037-24

Introduction

Methods of fluorescence spectroscopy are currently widely used in biology, ecology, and biomedicine [1]. These methods are essential in the study of interaction of small molecules with biopolymers, in microscopy and in sensitive quantitative analysis. At the same time, manipulation of spontaneous fluorophore emission is of great interest in these and many other optical applications (miniature lasers, light-emitting diodes, solar cells). Among potential approaches to control spontaneous emission of fluorophores is to modify the photonic local density of states in their nearest medium [2].

In recent decades, progress has been made in the development of various optical media capable of effectively manipulating the photonic local density of states and, consequently, the fluorescence. These include plasmon metamaterials [3,4], whispering gallery microresonators [5], photon crystals [6,7].

The photon crystals (PC) are themselves the artificial heterogeneous structures, that may be designed and fabricated in one- (1D), two- (2D) and three- (3D) dimensional geometry to control the propagation of light in a specific frequency band called the photonic band gap (PBG) [8]. One-dimensional PCs, where PBG represents itself a frequency band within which the light propagating in certain directions exponentially goes down, attract much attention both, from the standpoint of fundamental studies of light interaction with a matter [9,10], and from the standpoint of their practical application in the new generation advanced optoelectronic devices [11,12]. They have become a popular platform for implementing various efficient sensors based on fluorescent molecules for measuring biomolecular interactions, in particular for determining nucleic acids, detecting and studying the spectral properties of proteins, and monitoring of steroids behavior [13,14]. In paper [14] a possibility of protein fluorescence spectra control using PBG was demonstrated.

The spectral and fluorescent characteristics of dye molecules and the transfer of electron excitation energy between them in one-dimensional photon crystals were studied in [15,16]. Higher efficiency of electron excitation energy transfer in PC has been demonstrated.

The concept of controlling spontaneous emission by modifying the photon density of states in PCs has attracted considerable attention in the last decade. In this case, the key issue is whether the photon crystals can change the dynamics of spontaneous emission of the dye molecules [17,18]. In [19] the rate of spontaneous emission of fluorophores was controlled using organic molecular films with Lorentzian dispersion. This dispersion leads to an increase and decrease in the rate of photoluminescence attenuation at different wavelengths.

In [20], an increase in the rate of quantum dots spontaneous emission inside a porous silicon microresonator and an increase by almost a magnitude in the quantum dots photoluminescence intensity in the mode of weak coupling of light with a matter has been experimentally shown. The authors of [20] demonstrated a drastic change in the intensity of quantum dots spontaneous emission on the edge of PBG in distributed Bragg reflectors made of

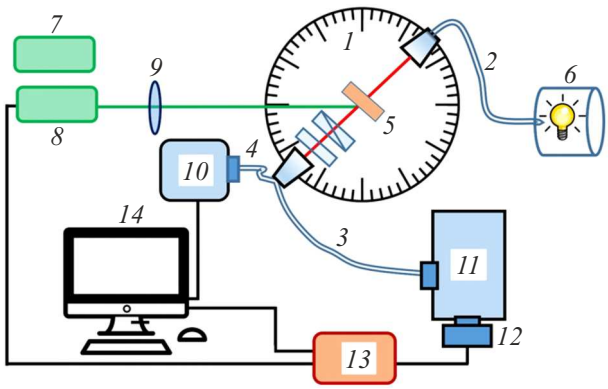

Figure 1. Schematic diagram of the system: *1* — rotary table, *2–4* — light guides, *5* — sample holder, *6* — white LED, *7, 8* — lasers, *9* — collective lens, *10* — spectrophotometer, *11* — monochromator, *12* — detector, *13* — single photons counter, *14* — computer.

porous silicon and proved its dependence on variations in the photonic states density.

This paper presents the results of studying the spectral characteristics and kinetics of fluorescence decay of acridine orange (AO) in one-dimensional PC arrays of mesoporous silicon.

Materials and methods

One-dimensional PCs based on oxidized mesoporous silicon (hereinafter referred to as PC) and samples of oxidized mesoporous silicon with a constant pore diameter (hereinafter referred to as PS) were used for the study. Average radii of pores in PC and PS, measured by gas sorption method, were 5.3 and 3.5 nm, respectively. The samples were prepared according to method described in [21]. The characteristics of PC layers (thickness and refractive index) were determined from the reference single-layer PS samples fabricated under the same conditions. The thicknesses of PCs layers, defined in this way are 85 ± 9 and 116 ± 9 nm, refractive indices are 1.46 and 1.33, and the number of periods in the structure is 100.

AO, which is an effective photosensitizer in the photo activated treatment, was selected for the study [22]. Maximum of its fluorescence spectrum coincides with PBG spectrum. Moreover, AO has a quite high quantum yield of fluorescence ($\eta = 0.46$) [22]. Despite of radiation quenching because of the luminophores contact with the surface of porous silicon, the incandescence intensity remains sufficiently high, which ensures its reliable recording. The samples were doped with the molecules of dye from ethanol solutions (96%). AO concentration was $4 \cdot 10^{-5}$ mol/l.

The studies were carried out using a system (Fig. 1) that allows measuring transmission spectra at different angles of light incidence on a sample, as well as measuring the luminescence spectra and luminescence kinetics at different recording angles.

The system consists of a rotary table (*1*) where the edges of three light guides are secured (*2–4*). Sample holder is placed in the center of the table (*5*). To measure the transmission spectra the white LED is used as a light source (*6*). The luminescence of the sample is excited by lasers (*7, 8*) with a wavelength of 405 nm, the light from which is focused on the sample using a collecting lens (*9*). A continuous semiconductor laser with a wavelength of 405 nm (*7*) was used to study the stationary fluorescence spectra. To study the fluorescence kinetics the pulse laser BDL-405 (wavelength 405 nm) (*8*) with a pulse duration of 80 fs was used. The spectra of transmission and steady luminescence were recorded by the spectrophotometer (*10*) on the basis of CCD matrix (3B Scientific GmbH). To measure the luminescence kinetics the recording light guide was connected to the input of the monochromator (*11*) (SOLAR TII MS2004), where photodetector PMC-100 (*12*) was installed at the output. Recording of luminescence kinetics is carried out using time-correlated counter of single photons (*13*) (Becker & Hickl GmbH). The measured full width at half maximum of the function was 200 ps. The pulse repetition frequency was 20 MHz. A slot width of the monochromator was 5 nm. Experimental system was controlled through a computer (*14*).

Findings and discussion

Spectral and fluorescent characteristics of the studied structures. Fig. 2 shows the transmission spectra of PS (curve *1*) and PC (curves *2–6*) for different angles of incident light. The transmission spectrum of PS (curve *1*) in the studied wavelengths practically does not change, while in PC (curves *2–6*) at different angles of incident light, non-monotonic dependences of transmission coefficients on wavelength are observed with a minimum (they have PBG)

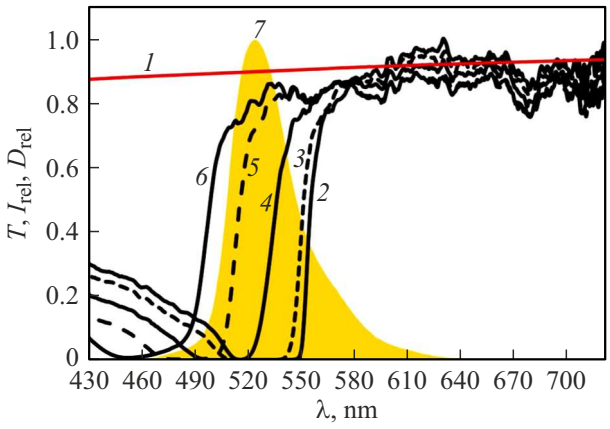

Figure 2. Transmission spectra: PS (*1*) and PC (*2–6*) at various incident angles of light: 0° (*2*), 5° (*3*), 10° (*4*), 15° (*5*), 20° (*6*). *7* — regulated fluorescence spectrum in AO at light incident angle 0°.

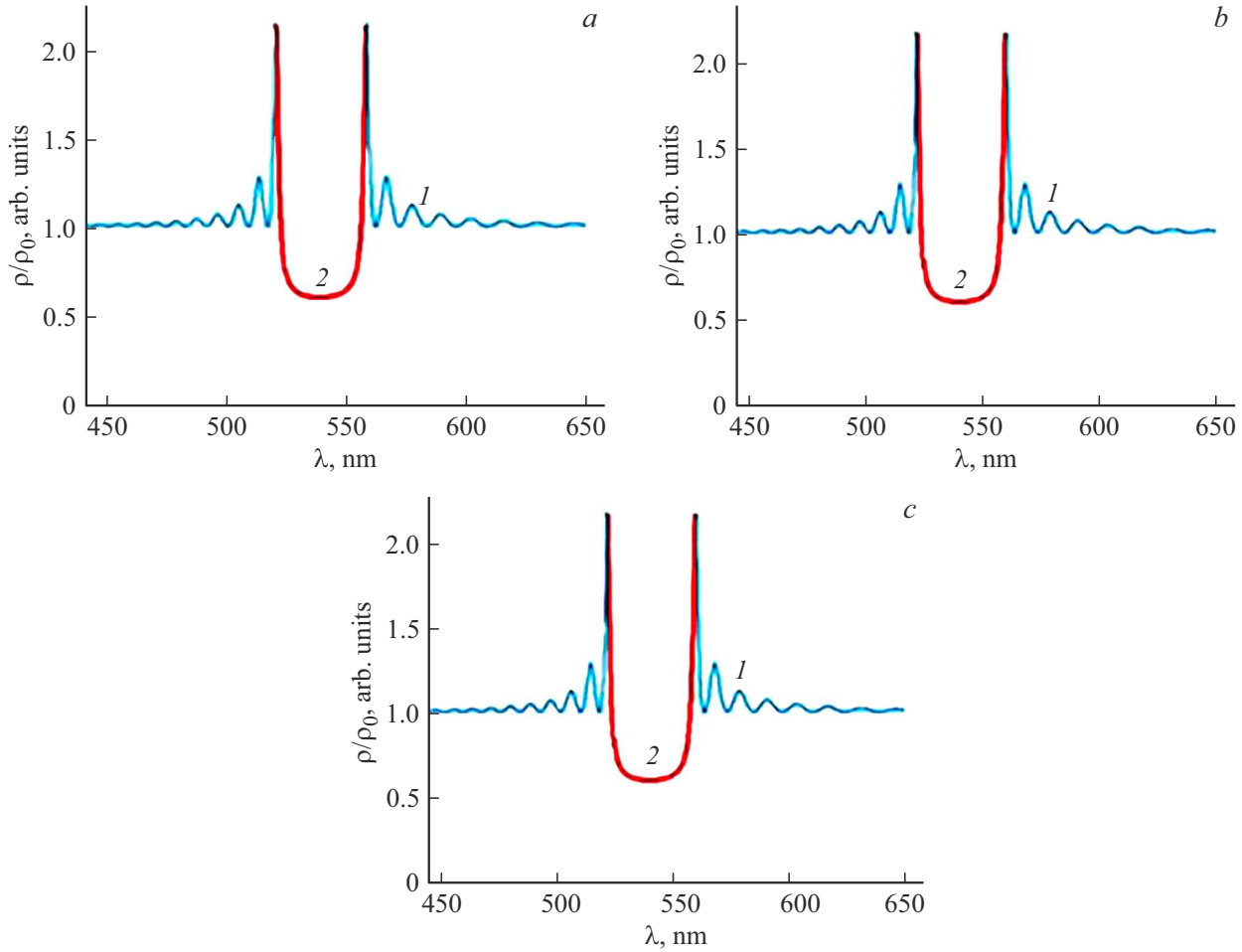

Figure 3. Density of EM modes in PC (101 layer, thickness 10 μm) with parameters $n_1 = 1.33$, $n_2 = 1.46$, $d_1 = 111$ nm, $d_2 = 84$ nm, TM-polarization at different light propagation angles (*a*) 0°, (*b*) 10°, (*c*) 15°. In all graphs curve *1* — density of the propagating EM modes, curve *2* — density of the evanescent EM modes.

in the wavelength range of ~ 30 nm, while spectral position of PBG varies depending on the angle of incident light.

To analyze the experimentally detected changes in the spectra and kinetics of AO fluorescence decay in PC (Figs. 4 and 5), it is necessary to estimate the distribution of the local density of electromagnetic (EM) field in PC. This may be accomplished with the use of dipole approximation. The reflectivity spectrum of the final PC was calculated using the method of propagation matrices [23]. After calculation, the complex reflectivity spectrum was reduced to the following form

$$r(\lambda) = r_0(\lambda)e^{i\phi(\lambda)}.$$

The reflectivity phase defined the phase of the reflected wave used to calculate the derivative $\left|\frac{\partial\omega}{\partial k}\right|$, where ω and k — frequency and wave vector of the photon inside PC, respectively. This is consistent with the group light velocity in PC. The density of EM mode states in PC was calculated according to the expression

$$\rho(\omega) = \frac{1}{2\pi}\frac{1}{\left|\frac{\partial\omega}{\partial k}\right|}.$$

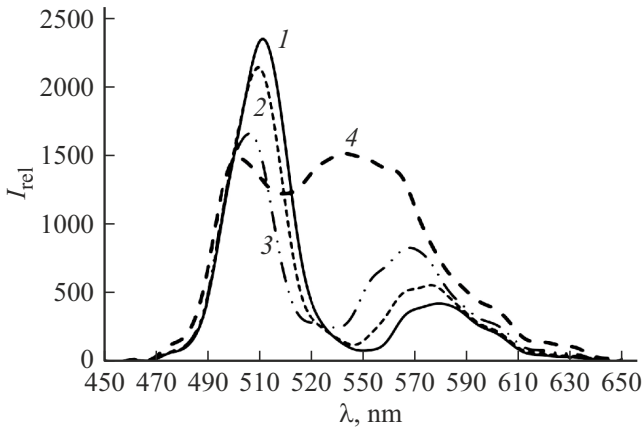

Figure 4. AO and PC fluorescence spectra when recorded at angles: $\alpha = 0°$ (*1*), 5° (*2*), 10° (*3*), 15° (*4*).

Since the wave vector in PC has real and imaginary parts, the density of EM modes can also classified as the density of propagating and evanescent modes.

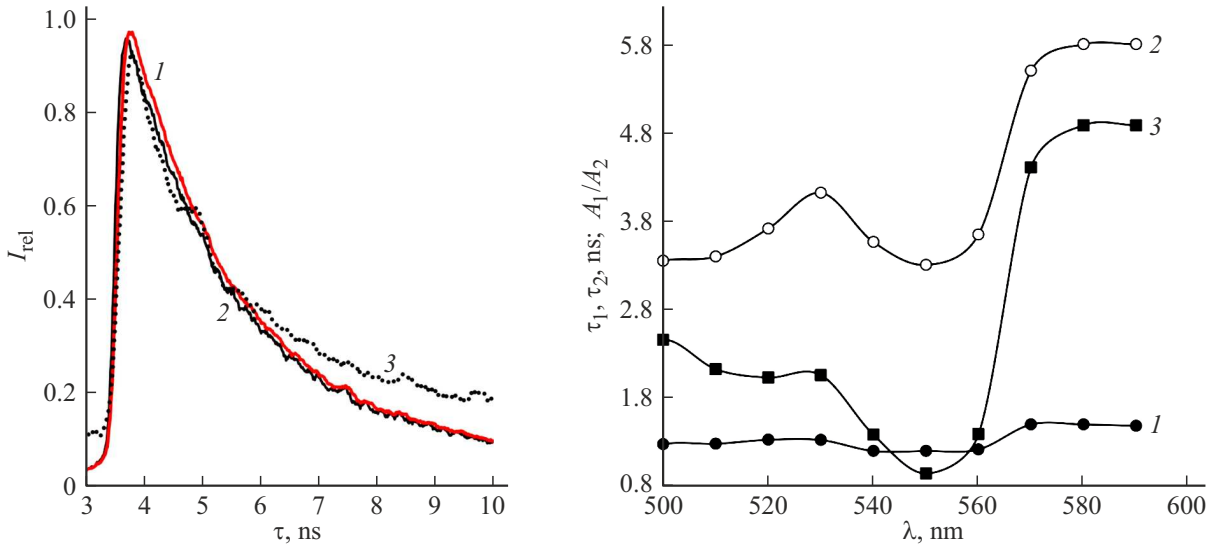

Figure 5. (*a*) AO molecules fluorescence intensity variation versus time in PS (*1*) and PC (*2, 3*) when recording at the wavelength of 510 (*1, 2*) and 550 nm (*3*). Excitation wavelength 405 nm. (*b*) Dependencies τ_1 (*1*), τ_2 (*2*) and A_1/A_2 for AO in PC on the wavelength at $\alpha = 0°$.

Fig. 3 illustrates the dependencies $\rho/\rho_0(\lambda)$ for the propagating (curve *1*) and evanescent (curve *2*) EM modes for various angles of TM-polarization light propagation. The curves are normalized for ρ_0 — density of EM-modes in isotropic medium with a refractive index n_{ef}, where

$$n_{ef} = n_1 \frac{d_1}{D} + n_2 \frac{d_2}{D}$$

is defined as an average weighted refractive index of PC layers (D — period of PC, d_1 and d_2 — thicknesses of layers).

It can be seen from the graphs that as the direction of light propagation deviates from the normal, the PBG shifts to the region of short wavelengths. The density of propagating modes goes to infinity on the edge of PBG, decreases when moving away from PBG boundaries and is minimal inside PBG. The density of the evanescent modes differs from zero only inside PBG, and approaches infinity on the edges of PBG. Therefore, total density of EM modes is minimal only in the center of PGB.

It is known [24] that the energy density of the incident EM wave is distributed unevenly across the PCs layers and depends on the frequency (wavelength). The energy density of a wave with a length more than PBG is concentrated in layers with a higher refractive index, and, conversely, the energy density with a wavelength less than the PBG is concentrated in layers with a lower refractive index. Consequently, we may expect a change in the spectral-fluorescent characteristics of the dye molecules that have been doped in PC.

AO fluorescence spectra in PC were measured at different angles α of luminescence recording. Fig. 4 illustrates AO fluorescence spectra in PC for several angles α.

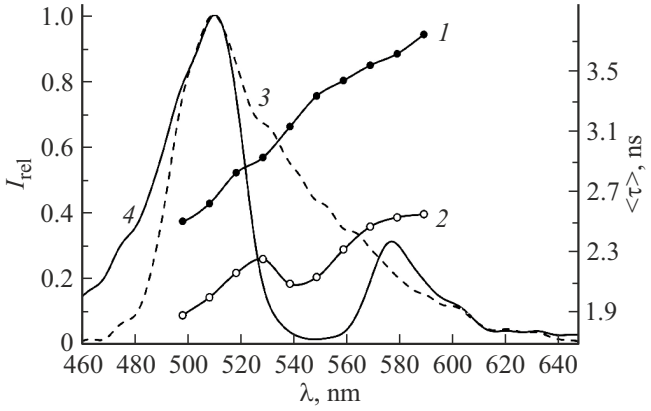

Figure 6. Curves of $\langle\tau\rangle$ for PS (*1*) and PC (*2*) versus recording wavelength. AO fluorescence spectra in PS (*3*) and PC (*4*) at observation angle $\alpha = 0°$.

From Fig. 4 we see that there's a „drop" caused by PBG in all fluorescence spectra. With an increase in the detection angle the „drop " in the spectrum shifts to the shortwave region, similar to the shift of PBG in PC transmission spectra (Fig. 2) and density of EM waves (Fig. 3).

Time-dependent characteristics of AO in PC. Fig. 5, *a* shows the curves of AO fluorescence versus time ($I(t)$) in PS (*1*) and PC (*2, 3*) at various observed wavelengths: outside PBG (*1, 2*) and inside PBG (*3*). From Fig. 5, *a* it is evident that if measurements are made at the wavelength outside of PBG the dependencies $I(t)$ for PS and PC coincide (curves *1, 2*). When observing AO fluorescence at wavelengths corresponding to PBG, a deviation of I is observed at high values t. A good consistency with the experimental curves is provided by approximating the

fluorescence decay of AO in PC by the sum of two exponentials:

$$I(t) = A_1\, e^{(-t/\tau_1)} + A_2\, e^{(-t/\tau_2)}, \qquad (1)$$

where A_i — amplitude of exponents, τ_i — exponents decay time. Fig. 5, *b* shows dependencies of τ_1 (curve *1*) and τ_2 (curve *2*) on the fluorescence wavelength. From Fig 5, *b* we see that τ_1 is practically independent from λ, while for τ_2 a non-monotonic dependence on λ is observed with a minimum corresponding to the „drop" in the fluorescence spectrum (Fig. 4). This Figure also illustrates the curve ofA_1/A_2 ratio versus λ. It can be seen that the proportion of molecules with long-living luminescence is growing in PBG.

Further, to analyze the effect of PBG PC on the kinetics of fluorescence of the dye molecules, we will consider the average lifetime of fluorescence:

$$\tau = \langle\tau\rangle = \frac{A_2\tau_1 + A_2\tau_2}{A_1 + A_2}. \qquad (2)$$

Fig. 6 illustrates the curves of $\langle\tau\rangle$ for PS (*1*) and PC (*2*) versus luminescence wavelength. From Fig. 6 it can be seen that with higher λ for PS a monotonous growth of $\langle\tau\rangle$ in the fluorescence spectrum is observed (curve *3* — fluorescence spectrum of AO in PS). For $\langle\tau\rangle$ in PC a non-monotonic dependence $\langle\tau\rangle$ on λ is observed with a minimum coinciding with PBG PC (curve *4* in Fig. 4 — AO fluorescence spectrum in PC).

From the dependence of AO lifetime in PC, it can be seen that within 535–560 nm (for the detection angle 0°), there is a decrease in the lifetime of AO fluorescence $\langle\tau\rangle$, and when approaching this range from the left and right $\langle\tau\rangle$ is increasing. As shown above, the density of EM modes (propagating and evanescent) is maximal on the edges of the PBG, which leads to increased luminescence.

The spectral dependences of excited AO state lifetime in PC on the angle α of fluorescence recording were measured. Fig. 7 shows as an example the curves of $\langle\tau\rangle$

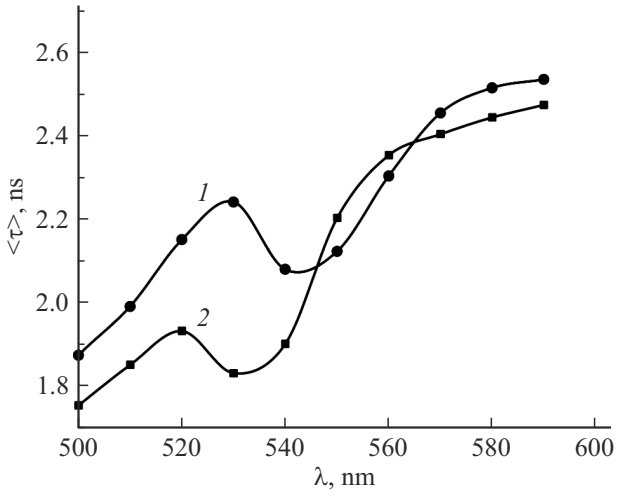

Figure 7. Curves of $\langle\tau\rangle$ versus the fluorescence wavelength at radiation detection angles. $\alpha = 0°$ (*1*), 15° (*2*).

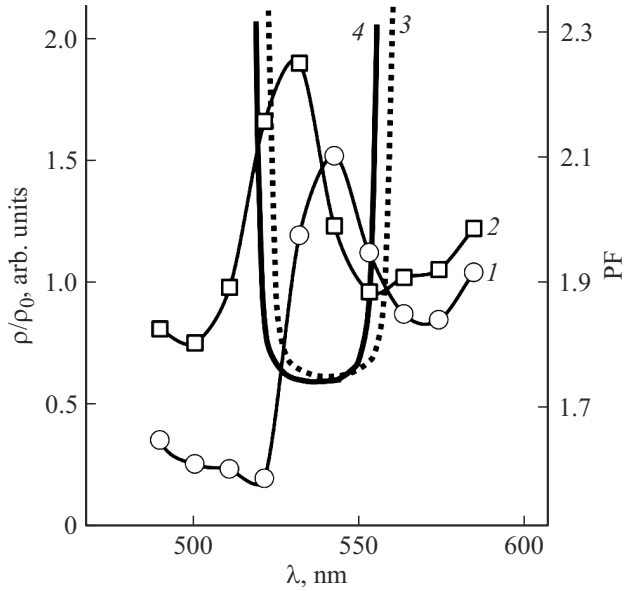

Figure 8. PF (*1, 2*) and ρ/ρ_0 (*3, 4*) versus λ for $\alpha = 0°$ (*1, 3*), 15° (*2, 4*).

versus luminescence wavelength for the two values $\alpha = 0°$ (curve *1*) and $\alpha = 15°$ (curve *2*). From Fig. 7 we see that an increase in α causes a shift of the „drop" in the non-monotonic dependence of $\langle\tau\rangle$ on λ to the shortwave region. While minima in the dependencies of $\langle\tau\rangle$ on λ coincide with the minima in the dependencies of ρ/ρ_0 on λ (Fig. 3).

Thus, the energy and time characteristics of AO fluorescence in one-dimensional photonic crystals differ for different wavelengths λ of their recording. The dependences of the fluorescence intensity and average lifetime of the excited state on the recording wavelength have a nonlinear nature with a „drop" at certain λ. Whereas the position of this „drop" depends on the angle of luminescence recording and coincides with the relative density of the photonic states of the EM field. Among potential approaches to describe the observed spectral dependences of the fluorescence intensity and average lifetime of the excited state of AO molecules in photonic crystals may be the Purcell effect (an increase in the oscillator emission rate in a resonator compared with the rate of spontaneous emission into free space).

Using the results of [20], let's calculate the values of the Purcell factor (PF) in photonic crystals for various fluorescence wavelengths and luminescence observation angles using formula

$$\mathrm{PF} = 1 + \left(\frac{\tau_0}{\tau_{\mathrm{PC}}} - 1\right)\frac{1}{\tau}, \qquad (3)$$

where PF — quantum yield of AO fluorescence inside PS; τ_0 — lifetime of excited state of AO molecules inside PS, τ_{PC} – lifetime of excited state of AO molecules inside PC.

Fig. 8 shows the curves of Purcell factor calculated from (3) versus wavelength for PC at $\alpha = 0°$ (curve *1*) and $\alpha = 15°$ (curve *2*). The same Figure also illustrates the

curves ρ/ρ_0 (curves *3, 4*). From Fig. 8 we see the growing PF in the region of PBG.

Conclusion

This study outlines the spectral dependences of the fluorescence intensity I and average lifetime $\langle\tau\rangle$ of the excited state of AO molecules integrated in one-dimensional photonic crystals at different angles of radiation detection. These dependences in PC samples were compared with equivalent samples with permanent pores. The density of EM evanescent and propagating modes in PC was calculated. The kinetics of AO fluorescence decay in PC for various wavelengths was analyzed. It is shown that spectral dependence of the average AO lifetime on the wavelength is contingent on the wavelength-dependent modified density of EM modes in photonic crystal. The Purcell factor for the studied systems was estimated.

Conflict of interest

The authors declare that they have no conflict of interest.

References

[1] D.-E. Zacharioudaki, I. Fitilis, M. Kotti. Molecules, **27**, 4801 (2022). DOI: 10.3390/ molecules27154801
[2] W.L. Barnes. J. Mod. Opt., **45**, 661 (1998). DOI: 10.1080/09500349808230614
[3] D. Semeniak, D.F. Cruz, A. Chilkoti, M.H. Mikkelsen. Adv. Mater., **35**, 2107986 (2023). DOI: 10.1002/adma.202107986
[4] A.D. Dmitriev, A.M. Saletskii. Opt. Spectrosc., **127** (2) 265 (2019). DOI: 10.1134/S0030400X19080095.
[5] T. Reynolds, N. Riesen, Al. Meldrum, X. Fan, J.M.M. Hall, T.M. Monro, A. François. Laser Photonics Rev., **11** (2), 1600265 (2017). DOI: 10.1002/lpor.201600265
[6] S. Wu, H. Xia, J. Xu, X. Sun, X. Liu. Adv. Mater., **30** (47), 1803362 (2018). DOI: 10.1002/adma.201803362
[7] Yu.A. Strokova, A.M. Saletsky. Opt. Spectrosc., **130** (12), 1545 (2022). DOI: 10.21883/EOS.2022.12.55240.3859-22.
[8] D.S. Sundar, T. Arun, R. Raju, K.S. Kumar, T. Sridarshini. *Photonic Crystal and Its Applications for Next Generation Systems* (Springer Nature, Singapore, 2023). DOI: 10/1007/978-981-99-2548-3
[9] P.S. Emeliantsev, N.I. Pyshkov, S.E. Svyakhovskiy. JETP Letters, **117** (11), 821 (2023). DOI: 10.1134/S002136402360129X
[10] S.E. Svyakhovskiy. JETP Letters, **118** (1), 26(2023). DOI: 10.1134/S0021364023601641.
[11] M. Gryga, D. Ciprian, L. Gembalova, P. Hlubina. Crystals, **13**, 93 (2023). DOI: 10.3390/cryst13010093
[12] S. Saravanan, R.S. Dubey. Nanosystems: Physics, Chemistry, Mathematics, **11** (2), 189 (2020). DOI: 10.17586/2220-8054-2020-11-2-189-194
[13] Y. Xiong, S. Shepherd, J. Tibbs, A. Bacon, W. Liu, L.D. Akin, T. Ayupova, S. Bhaskar, B.T. Cunningham. Micromachines, **14**, 668 (2023). DOI: 10.3390/mi14030668
[14] N. Zhdanova, A. Pakhomov, S. Rodionov, Yu. Strokova, S. Svyakhovskiy, A. Saletskii. Opt. and spectr., **128** (7), 909 (2020). DOI: 10.21883/OS.2020.07.49561.47-20 [N. Zhdanova, A. Pakhomov, S. Rodionov, Yu. Strokova, S. Svyakhovskiy, A. Saletskii. Opt. Spectrosc., **128**, 915 (2020). DOI: 10.1134/S0030400X20070267].
[15] Yu.A. Strokova, S.E. Svyakhovskii, A.M. Saletsky. Opt. Spectrosc., **125** (2), 208 (2018). DOI: 10.1134/S0030400X18080222.
[16] Yu.A. Strokova, S.A. Svyakhovskiy, A.M. Saletsky. J. Appl. Spectrosc., **85** (6), 1013 (2019). DOI: 10.1007/s10812-019-00752-1.
[17] H. Megahd, P. Lova, S. Sardar, C. D'Andrea, A. Lanfranchi, B. Koszarna, M. Patrini, D.T. Gryko, D. Comoretto. ACS Omega, **7**, 15499 (2022). DOI: 10.1021/acsomega.2c00167
[18] H. Megahd, M.V. Brito, A. Lanfranchi, P. Stagnaro, P. Lova, D. Comoretto. Mater. Chem. Front., **6**, 2413 (2022). DOI: 10.1039/d2qm00313a
[19] Kyu-Ri Choi, S. Li, D. H. Park, B. C. Joo, H. Lee, E.S.H. Kang, S.N. Chormaic, J.W. Wu, A. D'Aléo, Y.U. Lee. Nanophotonics, **13** (7), 1033 (2024). DOI: 10.1515/nanoph-2023-0631
[20] D. Dovzhenko, I. Vartynov, P. Samokhvalov, E. Osipov, M. Lednev, A. Chistyakov, A. Karaulov, I. Nabiev. Optics Express., **28** (15), 22705 (2020). DOI: 10.1364/oe.401197
[21] S.E. Svyakhovskiy, A.I. Maydykovsky, T.V. Murzina. J. Appl. Phys., **112** (1), 013106 (2012). DOI: 10.1063/1.4732087
[22] B. Fornaciari, M.S. Juvenal, W.K. Martins, H.C. Junqueira, M.S. Baptista. Photochem., **3**, 209 (2023). DOI: 10.3390/photochem3020014
[23] A. Luce, A. Mahdavi, F. Marquardt, H. Wankerl. JOSA A, **39** (6), 1007 (2022). DOI: 10.1364/JOSAA.450928
[24] J.D. Joannopoulos, S.G. Johnson, J.N. Winn, R.D. Meade. *Photonic Crystals: Molding the Flow of Light,* 2nd ed. (Princeton University Press, Princeton, 2011).

Translated by EgoTranslating